optic diffraction of guided optical waves in $LiNbO_3$," *Appl. Phys. Lett.*, vol. 23, pp. 417–419, 1973.
[39] P. K. Cheo, United Aircraft Research Laboratories, East Hartford, Conn., private communications.
[40] K. Ogawa, W. S. C. Chang, B. L. Sopori, and F. J. Rosenbaum, "A theoretical analysis of etched grating couplers for integrated optics," *IEEE J. Quantum Electron. (Part I of Two Parts)*, vol. QE-9, pp. 29–42, Jan. 1973.
[41] D. G. Dalgoutte, "A high efficiency thin grating coupler for integrated optics," *Opt. Commun.*, vol. 8, pp. 124–127, 1973.
[42] W. S. C. Chang, "Periodic structures and their applications in integrated optics," *IEEE Trans. Microwave Theory Tech. (1973 Symposium Issue)*, vol. MTT-21, pp. 775–785, Dec. 1973.
[43] E. A. J. Marcatillis and R. A. Schmeltzer, "Hollow metallic dielectric waveguides for long distance optical transmission and lasers," *Bell Syst. Tech. J.*, vol. 43, pp. 1783–1809, 1964.
[44] T. J. Bridges, E. G. Buckhardt, and P. W. Smith, "CO_2 waveguide lasers," *Appl. Phys. Lett.*, vol. 20, pp. 403–405, 1972.
[45] R. E. Jenson and M. S. Tobin, "CO_2 waveguide laser," *Appl. Phys. Lett.*, vol. 20, pp. 408–510, 1972.

GaAs and GaAlAs Devices for Integrated Optics

VIKTOR EVTUHOV, MEMBER, IEEE, AND AMNON YARIV, FELLOW, IEEE

(Invited Paper)

***Abstract*—The emergence of a monolithic optical circuit technology depends on the availability of materials capable of performing complex electrooptic functions and on the development of new fabrication techniques. The work done on GaAs and its related alloys is reviewed and summarized, and their feasibility for integrated optical circuits is examined.**

I. INTRODUCTION AND CHRONOLOGICAL REVIEW

THE FIELD of integrated optics has as its professed goal the eventual fabrication of complex optical circuits in small solid configurations. Such circuits will become necessary if the many hopes for optical communication and optical computers are ever to come true.

The main motivation for this work derives from the spectacular success of integrated electronics where a single "mother" material—silicon—is used to fabricate extremely complex circuits.

Although the nature of optical interactions is such that we are not likely to approach the component density of integrated electronics, the inherent simplicity and reliability of single crystal circuits is reason enough to strive for optical monolithic circuits.

In this paper we will review a series of experimental and theoretical developments which took place during the period 1966–1974. These experiments have to do mostly with establishing the feasibility of performing some key optical functions in GaAs and GaAlAs crystal systems.

The interest in GaAs as a basic material for optical integrated circuits (OIC) has been stimulated by the fact that this material has a high degree of versatility in terms of its electrical and optical properties and is potentially suitable for fabrication of a variety of necessary optical circuit components. This is especially true if one considers the possibility of alloying GaAs with Al producing a ternary compound of the form $Ga_{1-x}Al_xAs$. Because the optical transmission characteristics of $Ga_{1-x}Al_xAs$ are strongly dependent on x, this material is easily tailored to allow waveguiding of various near IR wavelengths. For example, by varying x between zero and 0.3, the band edge of the compound is shifted from 9000 to 7000 Å. This will be discussed in more detail in Section II. GaAs also has high electrooptic, acoustooptic, and optical nonlinear coefficients, making it potentially applicable to a variety of switching, modulation, and frequency conversion devices. Finally, it is compatible with a number of fabrication techniques such as ion implantation, epitaxial growth, and electron beam and ion micromachining. Light-emitting diodes (LED's), lasers, modulators, switches, and detectors can be fabricated using this material. The most important properties of GaAs and $Ga_{1-x}Al_xAs$ are summarized in Table I.

GaAs and GaAlAs possess most of the properties needed to perform complex optical functions and thus hold promise for the development of monolithic optical circuits in which all the components are fabricated using basically the same material on a single chip substrate. However, the components being developed at this time in various laboratories are not tied exclusively to the monolithic circuit approach and are compatible with the "hybrid" approach where different materials are used to perform different

Manuscript received April 19, 1974. This work was supported in part by the Air Force Cambridge Research Laboratories and the Advanced Research Projects Agency and in part by the Office of Naval Research and the Army Research Office.

V. Evtuhov is with Hughes Research Laboratories, Malibu, Calif.
A. Yariv is with the Department of Electrical Engineering, California Institute of Technology, Pasadena, Calif. 91125.

TABLE I
PROPERTIES OF GaAs, GaAlAs, AND RELATED ALLOYS

Transparency	0.7 μm - 12 μm
Interfacing with Electronic Circuits	Ohmic Contacts, Doping, and Junction Technology Highly Developed
Light Generation	Used in p-n Junction Lasers
Application to Switching Devices	Among the largest electro-optic and acousto-optic figures of merit $n_o^3 r_{41} \simeq 6\times10^{-11}\ \frac{m}{V}$, $M \equiv \frac{n^6 p^2}{\rho v_s^3} \simeq 10^{-13}$
Thin Films Fabrication Techniques	Epitaxy, doping, ion implantation
Applicability to Nonlinear Devices	One of the best nonlinear optical materials $d_{NL} \simeq 10^{-21}$(MKS)

functions. This approach may become necessary if it is shown that transmission losses in $Ga_{1-x}Al_xAs$ cannot be reduced below a few decibels per centimeter. The question of the magnitude of the propagation loss in $Ga_{1-x}Al_xAs$ optical waveguides at various wavelengths is still an unanswered question. It is discussed in somewhat more detail in the next section.

The most likely operating wavelengths for OIC's appear to be in the near IR (0.7–1.1 μm) because of the good transmitting characteristics of glass optical fibers in this wavelength region, the promise of practical easily integrated semiconductor sources, and the availability of high quantum efficiency room temperature detectors. However, the existence of high-power tunable capillary CO_2 laser sources [1] makes it important to consider the 10.6-μm wavelength as well. Thus several workers are now investigating GaAs and $Ga_{1-x}Al_xAs$ specifically from the point of view of 10-μm applications.

The interest in GaAs as an optical material can be traced to 1962 when the second named author and R. Leite, then at the Bell Laboratories, were trying to understand the reason for the observed low loss of the newly discovered GaAs junction lasers [2], [3]. The observed output beamwidth of a few microns would have, in an ordinary laser, caused extremely large diffraction losses, of the order of $\alpha \simeq 1000\ cm^{-1}$. The measured threshold indicated losses, at least an order of magnitude smaller. In a jam session involving R. Kompfner it was decided, for lack of better alternatives, to invoke the mechanism of dielectric waveguiding. This guiding, which takes place when a dielectric layer is sandwiched between media of lower index of refraction, was assumed to overcome the effect of diffraction thus keeping the losses to the observed low values. An analytic check of this hypothesis [4] showed that the amount of index discontinuity Δn necessary to support the lowest mode is given by

$$\Delta n > \frac{1}{8n}\frac{\lambda_0^2}{t^2} \tag{1}$$

where t is the guide height. Since the wavelength λ_0 in GaAs is $\sim$0.85 μm, $n \sim 3.5$, and the thickness t was a few microns, (1) predicts that a minute difference of $\Delta n \simeq 10^{-3}$ is enough to explain the observed guiding. It was felt that it was not unreasonable to assume that a small index curvature of the right sign could accompany the strong chemical transition from p to n doping and give rise to guiding. To check this hypothesis an attempt to look for guiding in nonlasing p-n GaAs diodes was made and, indeed, in an experiment together with Bond and Cohen, such guiding was observed [5].

The next advance in this field came when Nelson and Reinhart used a reverse biased pn junction in GaP both as a waveguide and a modulator [6]. Taking advantage of the large electric field in the depletion region of the junction and of the electrooptic properties of GaP, they demonstrated modulation of light guided in the junction plane. As in the earlier [4], [5] work, the exact nature of the physical mechanism responsible for the index profile was not clearly established. Although the experiment was performed in GaP and in a naturally occurring waveguide, it established the feasibility of combining two functions—guiding and modulation in a single crystal.

Since the optical confinement in the GaAs laser diodes was shown to lead to a reduction in the threshold, it seemed logical that a deliberate control of the index profile should lead to better confinement and lower thresholds. The first successful realization of this scheme was that of Alferov and his coworkers in Leningrad [8].

By growing heterojunctions of GaAlAs–GaAs–GaAlAs and taking advantage of the lower index of refraction of GaAlAs compared to GaAs they were able to confine the laser mode to the active (amplifying) GaAs inner layer. Refinements of these ideas [9], [10] led eventually to CW junction lasers operating at room temperature.

These early experiments demonstrated the ability of semiconductor p-n junctions to generate, guide, and modulate light. It also became clear that guiding and control of light can occur not only in buried waveguides but in guides fabricated on the surface of the semiconductor.

In 1966, Hall, then a first year graduate student at Caltech, started looking for guiding in a surface layer of GaAs. Three years later, using an epitaxial film of lightly doped GaAs on a heavily doped substrate he observed the guiding and demonstrated electrooptic modulation in GaAs films [11], [12].

The collective efforts of many investigators who were trying to guide and manipulate light in thin films was given in 1969 the name integrated optics by Miller [13]. In March 1971 this new field was given its official kickoff by the first (one day) conference on "Guiding and Processing of Optical Waves in Thin Films." Describing the recent Caltech results in GaAs, Yariv suggested that this material could form the basis of a monolothic approach to fabricating integrated optical circuits.

The initial success of guiding and modulating in GaAs led to a joint Caltech–Hughes Laboratories research effort in which additional optical functions including detection, directional coupling, and distributed feedback lasers in GaAs were explored. A review of this work constitutes the major part of the following report.

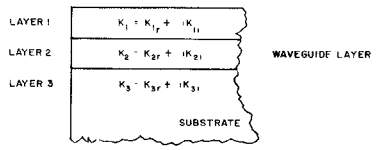

Fig. 1. Schematic representation of a three layer slab dielectric waveguide.

II. GaAs AND GaAlAs OPTICAL WAVEGUIDES

To fabricate a planar optical waveguide it is necessary to produce a thin layer which has a higher index of refraction than the surrounding media. Thus a typical planar thin film waveguide configuration is as shown in Fig. 1. In the figure, K_1 K_2, and K_3 are the relative dielectric constants (i.e., $K = n^2$ with n being the complex index of refraction). The fact that the media are in general lossy is accounted for by taking the K's as complex numbers as shown in the figure. Most commonly the top layer is omitted and the waveguide layer–air interface forms the upper boundary of the guide. In this case $K_{1i} = 0$ and $K_{1r} = 1$. Under these circumstances the condition for propagation of the first m modes in a waveguide of height t is [14]

$$2n(n_2 - n_3) > \left(\frac{m\lambda_0}{4t}\right)^2, \qquad m = 1,3,5,\cdots. \tag{2}$$

The mode designation $m = 1,3,5,\cdots$ is inherited from that of a symmetric waveguide. The mode $m = 1$ is the lowest order propagating mode in the waveguide of Fig. 1 with air as the top layer while $m = 3$ is the next higher mode. The even modes $m = 0$ and $m = 2$, etc., which exist in a symmetric guide do not exist in this guide. From the preceding formula it can be seen that for $t \simeq \lambda_0$, $\Delta n \sim 10^{-2}$ is required for guiding.

There are several methods which can be used to fabricate planar waveguides in GaAs and $Ga_{1-x}Al_xAs$. The most important ones are epitaxial growth of impurity doped layers with different impurity concentrations (and therefore different indices of refraction), heteroepitaxial growth of $Ga_{1-x}Al_xAs$ layers of varying Al concentration, and reduction of carrier concentration in the guiding layer produced by ion implantation, proton bombardment, or diffusion doping. The last two methods (heteroepitaxy and carrier concentration reduction) have so far been the most commonly employed methods for producing planar waveguides.

The carrier concentration reduction method for waveguiding [11] is based on the fact that the presence of free carriers in semiconductors causes a decrease of the refractive index. The index change is related to the number of free carriers by the following relation:

$$2n(\Delta n) = \frac{-\Delta N e^2}{\epsilon_0 m^* \omega^2} \tag{3}$$

where ϵ_0 is the permittivity of free space. ΔN is the free carrier concentration difference between layers, m^* is the carrier effective mass (assumed the same in both layers), ω is the optical frequency, and e is the electronic charge. With $m^* = 0.068m$ for GaAs (m is the free electron mass) $\Delta N = 10^{18}$ cm^{-3} gives an index difference of about 1.7×10^{-3} for optical wavelengths of about 1 μm.

A. Proton Implanted Waveguides

The use of proton implantation for the formation of planar optical waveguides in GaAs has been demonstrated by Garmire *et al.* [15]. In their experiments they started with a relatively heavily doped n-type GaAs substrate material and then formed a compensated layer ($\sim$3 μm thick) of low carrier concentration by proton bombardment which creates deep carrier-trapping levels (see Fig. 2). Resistivity in the compensated layer was $\sim 10^7$ Ω·cm, corresponding to a carrier concentration of $\sim 10^8$ cm^{-3} immediately following implantation (increasing after annealing). The thickness of the layer depends on the proton energy and is roughly 1 μm for each 100 keV of proton energy [16]. Proton dose is typically $\sim 10^{15}$/cm^2. Waveguides formed by proton bombardment of GaAs have the disadvantage that there is considerable optical absorption at wavelengths longer than the bandgap wavelength due to excitation of carriers out of the traps. This absorption can be reduced to acceptable levels ($\alpha \sim 1$ cm^{-1}) by annealing at temperatures in the range 250–600°C to reduce the number of traps to the absolute minimum required to produce the compensated layer.

The optical mode shape and the attenuation loss for 1.15-μm wavelength light in planar waveguides as functions of proton dose, and of anneal temperature and duration were measured by Garmire *et al.* [15] who found the lowest value of loss to be 2 cm^{-1}. The least attenuation observed subsequently is approximately 3.7 dB/cm ($\alpha = 0.8$ cm^{-1}), in a sample with substrate concentration $N = 1.9 \times 10^{18}$/cm^3 which was implanted with a 300-keV proton dose of 2×10^{15} cm^2 and annealed for 1 h at 500°C [11]. There is evidence to suggest that at least part of the observed attenuation results from free carrier absorption of photons in the "tail" of the mode which extends into the substrate. The optical mode shape has been found to depend on substrate carrier concentration, proton dose, and anneal conditions. In samples with very large substrate carrier concentrations ($N_s \geq 6 \times 10^{18}$/cm^3) both TE_0 and TE_1 mode propagation was observed, while in samples with $N_s < 6 \times 10^{18}$/cm^3 only the TE_0 mode is supported (see Fig. 3). These observations are in agreement with calculations based on (2) and (3. The shape of the optical mode has been observed to broaden after annealing, because of changes in the carrier concentration profile [18] (see Fig. 4).

The role of postimplantation annealing in reducing the propagation losses (at $\lambda_0 = 1.16$ μm) is illustrated by Fig. 5.

Fabrication of waveguides by diffusion of impurities is, in principle, similar to the proton bombardment technique. However, the bombardment technique generally yields a more sharply defined guide boundary.

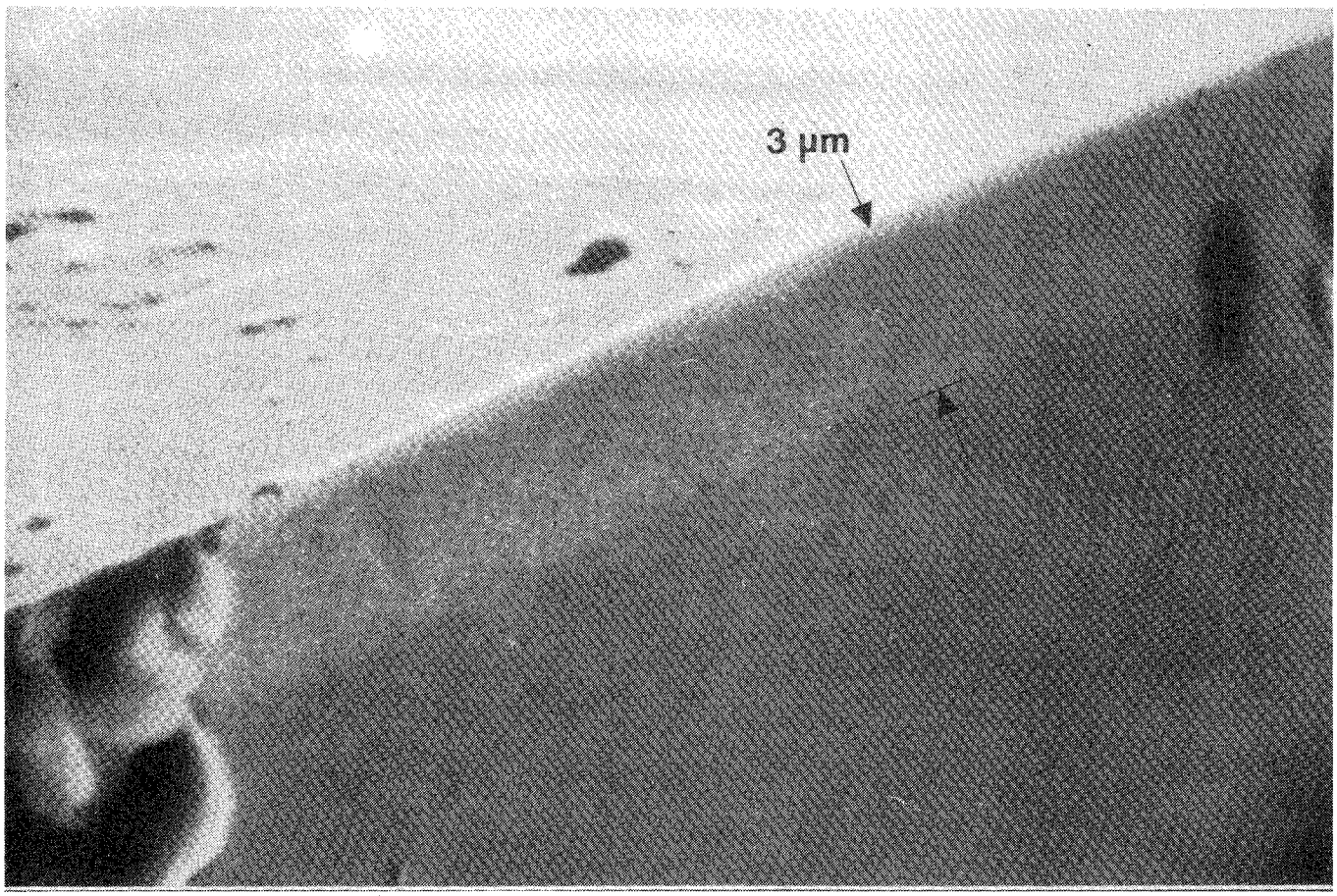

Fig. 2. Scanning electron micrograph of an ion implanted dielectric waveguide in GaAs.

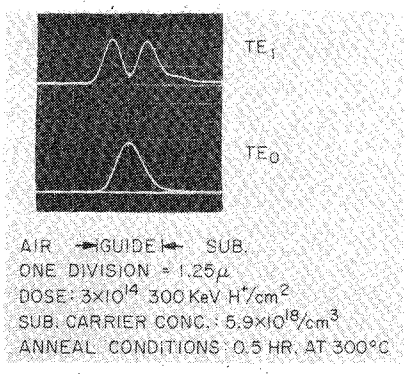

Fig. 3. Intensity mode profile of the TE_0 and TE_1 mode of the waveguide shown in Fig. 2. After [15].

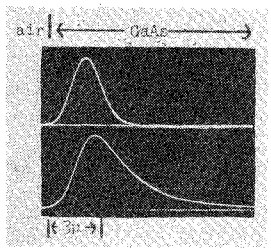

Fig. 4. Change in confinement of an ion implanted waveguide due to annealing. After [15].

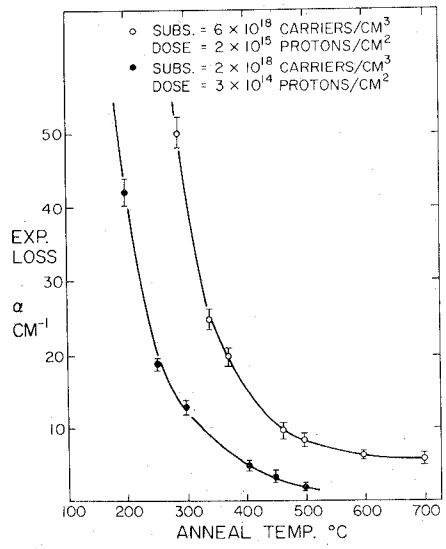

Fig. 5. The dependence of optical losses at $\lambda_0 = 1.15$ μm of an implanted GaAs waveguide on annealing temperature. After [15].

B. Heteroepitaxial Waveguides

Formation of waveguides by the heteroepitaxial growth of $Ga_{1-x}Al_xAs$ layers is based on the dependence of the refractive index of the material on the Al concentration x. This dependence is shown in Fig. 6. (The latest measurements of this dependence were reported by Casey *et al.*

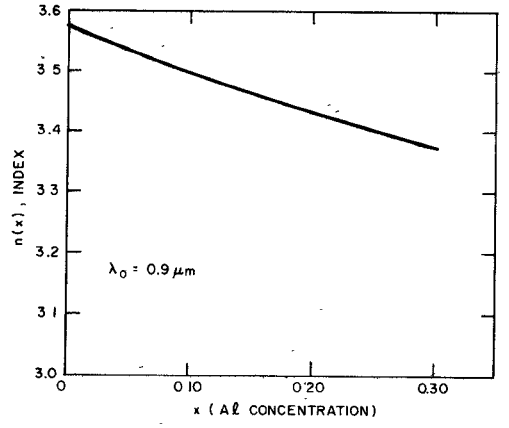

Fig. 6. The index of refraction of $Ga_{1-x}Al_xAs$ as a function of the molar fraction (x) of Al.

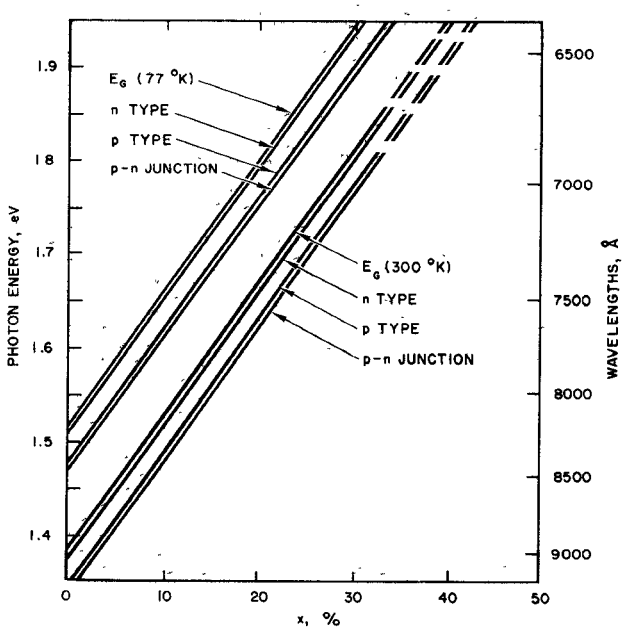

Fig. 7. The energy gap of $Ga_{1-x}Al_xAs$ versus x.

[19].) In addition, the presence of Al in GaAs shifts the absorption band edge, thus enabling one to produce waveguides with short wavelength transmission cutoff varying between $\lambda_0 \simeq 9500$ Å and $\lambda_0 \simeq 6500$ Å. The dependence of the band gap energy on the Al concentration (x) in $Ga_{1-x}Al_xAs$ determined by the luminescence wavelength is shown in Fig. 7 [20], [21].

One of the key issues in GaAs and $Ga_{1-x}Al_xAs$ waveguides is the nature of the loss mechanisms which will attenuate the propagating mode. Relating these mechanisms to material parameters and incorporating guide propagation considerations allow one to develop guidelines for waveguide fabrication. The most important sources of loss are: 1) band-to-band transitions, and 2) free carrier absorption. Loss caused by the first mechanism can be minimized by a proper choice of the energy gap relative to the operating wavelength. Free carrier loss will be present, however, since the impurity concentration, although kept to a minimum, is always finite.

The allowable impurity concentrations can be estimated by solving for the optical losses of the propagating modes as a function of the carrier concentrations in the substrate and the guiding layer. Consider a thin film waveguide such as illustrated in Fig. 1. We may assume conservatively, that the loss constant for the guide α_g is equal to the largest of the loss constants corresponding to the various layers, i.e.,

$$\alpha_g = \frac{k_0 \operatorname{Im} K}{(\operatorname{Re} K)^{1/2}} \tag{4}$$

where $k_0 = 2\pi/\lambda_0$ with λ_0 being the propagating wavelength and where the imaginary part of K(Im K) is taken as the largest of Im K_1, Im K_2 and Im K_3.

An expression for Im K can be derived from a simple treatment of the carrier polarization in the presence of collisions of lifetime τ. This gives

$$\operatorname{Im} K = -\frac{Ne^2/(m^*\epsilon_0\omega\tau)}{\omega^2 + 1/\tau^2} \tag{5}$$

where m^* is the effective mass, ϵ_0 is the dielectric constant of vacuum in MKS units, and N is the carrier density.

In GaAs using a mobility $\mu = 8.5 \times 10^3$ cm^2/V·s we have at $\lambda_0 = 1$ μm, $\tau = m^*\mu/e = 3.4 \times 10^{-13}$ s, $\omega = 2\pi f \cong 1.88 \times 10^{15}$, and $n = 3.51$. From (4) and (5) we obtain in the limit $\omega \gg 1/\tau$

$$\alpha_g = \left(\frac{\mu_0}{\epsilon}\right)^{1/2} \frac{Ne^2}{m^*\omega^2\tau} \tag{6}$$

where μ_0 is the permeability of free space and ϵ is the dielectric constant of the material. With the preceding data for GaAs we obtain

$$\alpha = 3.6 \times 10^{-19} N(\text{cm}^{-1}) \tag{7}$$

where N is in cm^{-3}.

In OIC's with typical dimensions of a few millimeters we should be able to tolerate $N < 10^{19}$ cm^{-3} at which point the loss in 1 mm should be $1 - e^{-0.36} \approx 0.30$. Because the experimental absorption [22] invariably runs higher than theoretical estimates the value $N \leq 10^{17}$ cm^{-3} is generally adopted as a design parameter for the maximum carrier concentration in the substrate or the guiding layer.

We now turn to the question of the aluminum concentration difference between the guiding layer and the substrate required for single mode propagation. This can be determined in a straightforward but somewhat approximate fashion by ignoring the slight nonlinearity in the dependence of the refractive index on Al concentration. We may thus assume the following relationship between layer–substrate index difference, $(n_2 - n_3)$ and Al concentration difference. Δx: $n_2 - n_3 \approx 0.4\Delta x$, where n_2 and n_3 are the guiding layer and the substrate indices of refraction, respectively.

Using the condition for propagation (2) and relating $(n_2 - n_3)$ to Al concentration difference Δx yields the

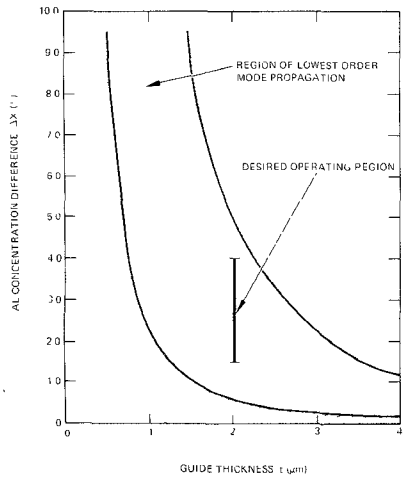

Fig. 8. Allowed region of the Al molar fraction x for single mode operation in $Ga_{1-x}Al_xAs$ as a function of guide thickness.

TABLE II
REFRACTIVE INDEX OF $GA_{1-x}AL_xAS$

Material	A	B	C	D
GaAs	10.906	0.97501	0.27969	0.002467
$Ga_{1-x}Al_xAs$	10.906 - 2.92x	0.97501	$(0.52886 - 0.735x)^2$ $x \leq 0.36$ $(0.30386 - 0.105x)^2$ $x \geq 0.36$	0.002467(1.41x + 1)

Note: $n^2 = A + (B/\lambda_0^2 - C) - D\lambda_0^2$.

condition for lowest order ($m = 1$) mode propagation

$$\frac{11.25}{n}\left(\frac{\lambda_0}{4t}\right)^2 > \Delta x > \frac{1.25}{n}\left(\frac{\lambda_0}{4t}\right)^2 \qquad (8)$$

where $n = (1/2)(n_2 + n_3)$. This relation can be used to plot the curves of Fig. 8, which give the ranges of guiding film thickness and aluminum concentration difference allowed for single mode propagation. Typically, for film thicknesses ranging between 1.25 and 2.5 μm the allowable Δx is approximately in the range of 1.5–3.5 percent.

A more accurate calculation (23) of the relationship between the film thickness and the Al concentration difference can be obtained by using the Sellmeir equation [24] to estimate the refractive indices of $Ga_{1-x}Al_xAs$ for different values of x:

$$n(x) = A + \frac{B}{\lambda_0^2 - C(x)} - D(x)\lambda_0^2$$

where the coefficients A, B, C, and D are given in Table II.

The absolute level of Al concentration in the guiding layer can be estimated by considering the spectral location and shape of the $Ga_{1-x}Al_xAs$ absorption edge as a function of Al concentration and assuming a value for maximum allowable absorption coefficient due to interband transitions. Curves of Fig. 9 were plotted using available data for GaAs. The absorption edges shown for increasing Al concentrations were obtained by calculating the bandgap using the expression [21] $E_g(x) = 1.439 + 1.042x + 0.468x^2$ and then shifting the band edge of GaAs to correspond to the computed value $E_g(x)$. More detailed plot of the long wavelength tail of the band edge [25] with different abscissas corresponding to different Al concentrations is shown in Fig. 10. The required Al concentration was determined from these curves using an allowable value of absorption coefficient $\alpha = 2$ cm^{-1} (8.6 dB/cm) and $\alpha = 0.7$ cm^{-1} (3 dB/cm) and various possible source wavelengths which might potentially be used in OIC's. The

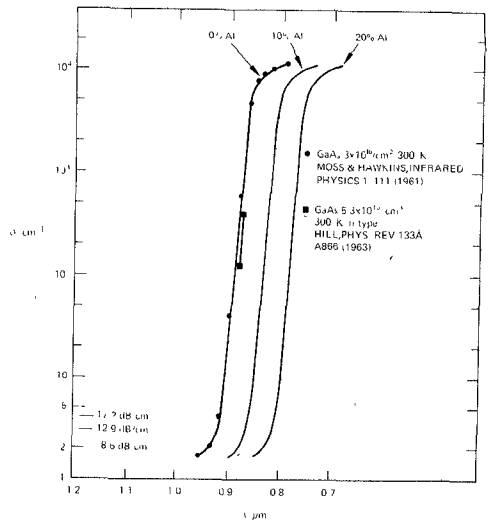

Fig. 9. The spectral dependence of the absorption in $Ga_{1-x}Al_xAs$ for $x = 0$, 0.1, 0.2.

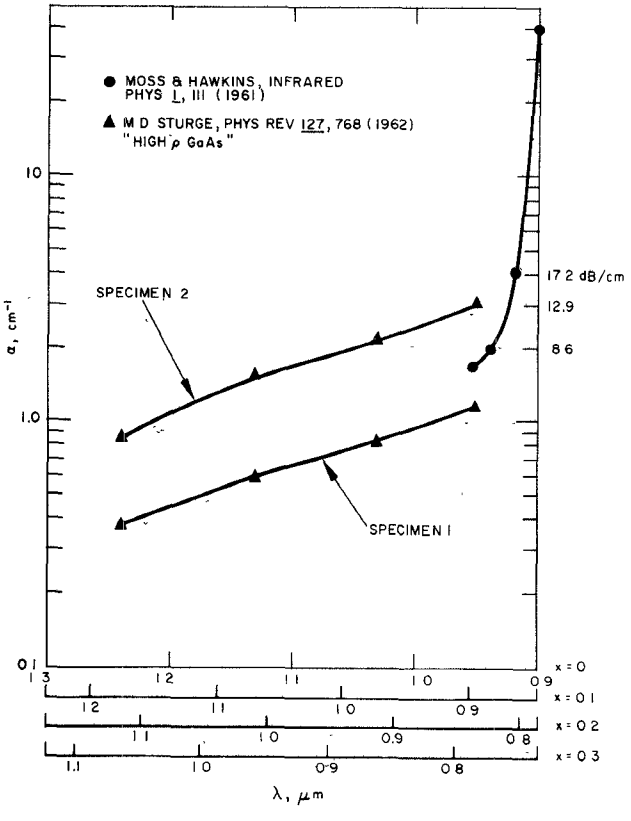

Fig. 10. Absorption near the bandgap of $Ga_{1-x}Al_xAs$ for $x = 0$, 0.1, 0.2, 0.3.

TABLE III
REQUIREMENTS ON ABSOLUTE AL CONCENTRATION

Source Wavelength	Req. Al Concentration in the Guide	
	α = 2 cm^{-1} (8.6 db/cm)	α = 0.7 cm^{-1} (3 db/cm)
0.85 μm GaAlAs	17%	40%
0.9 μm GaAs	7%	32%
0.95 - 1.0 μm Si:GaAs	0%	20%

Note: Substrate concentration ~3 percent higher. Material becomes indirect at 40-percent Al.

results are shown in Table III. It is seen that Al concentrations up to 40 percent may be required in extreme cases. In most cases lower Al concentration should be allowable. These results must be considered to be approximate since no accurate measurements of the actual loss coefficient in $Ga_{1-x}Al_xAs$ waveguides as opposed to bulk material are available.

At the present time several workers are engaged in heteroepitaxial growth of GaAs and $Ga_{1-x}Al_xAs$. Several methods of growth are being pursued including vapor phase epitaxy, slide-bar limited melt, and vertical dipping "infinite" melt liquid phase epitaxy. Standard techniques are generally used to evaluate the thin film electrical, chemical, and crystalline properties. These techniques include microprobe, photoluminescence, and x-ray analysis, Hall effect and C–V measurements, and scanning electron microscope examinations.

Some examples of the more recent work on the epitaxial growth of GaAlAs and $Ga_{1-x}Al_xAs$ for integrated optics applications can be found in papers by Craford and Groves [26], Garmire [27], and Kamath [28] as well as workers in the 10-μm field [29]–[38]. Craford and Groves investigated the vapor phase epitaxial growth of III–V compounds primarily for LED applications. Garmire's and Kamath's work is aimed more directly at producing optical waveguides for near IR applications. Garmire used liquid phase epitaxy to obtain low-loss $Ga_{1-x}Al_xAs$ waveguides on GaAs substrates. The guiding actually occurred near the top (air interface) of the $Ga_{1-x}Al_xAs$ layer in the region of Al concentration gradient (i.e., lower Al concentration near the surface). Such gradients are produced by using thin melts for the liquid phase epitaxy. Losses in these were measured to be <1 cm^{-1}. An example of a composite GaAs–GaAlAs waveguide is shown in Fig. 11.

In his work Kamath used a variety of epitaxial techniques. He has grown layers of $Ga_{1-x}Al_xAs$ with values of x ranging between zero and 0.7. He found that the commonly used limited melt or slide bar technique, while suitable for the growth of several layers in succession, has inherent limitations due to mixing problems and due to the high segregation coefficient of Al. These problems cause complications when thick large area layers are required. He has, therefore, pursued an "infinite" melt liquid epitaxy method to produce large area layers (1 in^2) with controlled thickness varying from 5 to 75 μm.

The work on GaAs waveguides at 10 μm has been directed primarily at developing structures for active devices such as modulators. These structures pose special problems because of the metallic electrodes which they require. The presence of the electrodes may introduce high attenuation in the guides due to the metal–dielectric boundary. Structures aimed at overcoming these problems have been analyzed by Chang and Loh [29], who have also developed some design guidelines for these structures. Experimental work on such structures has been reported

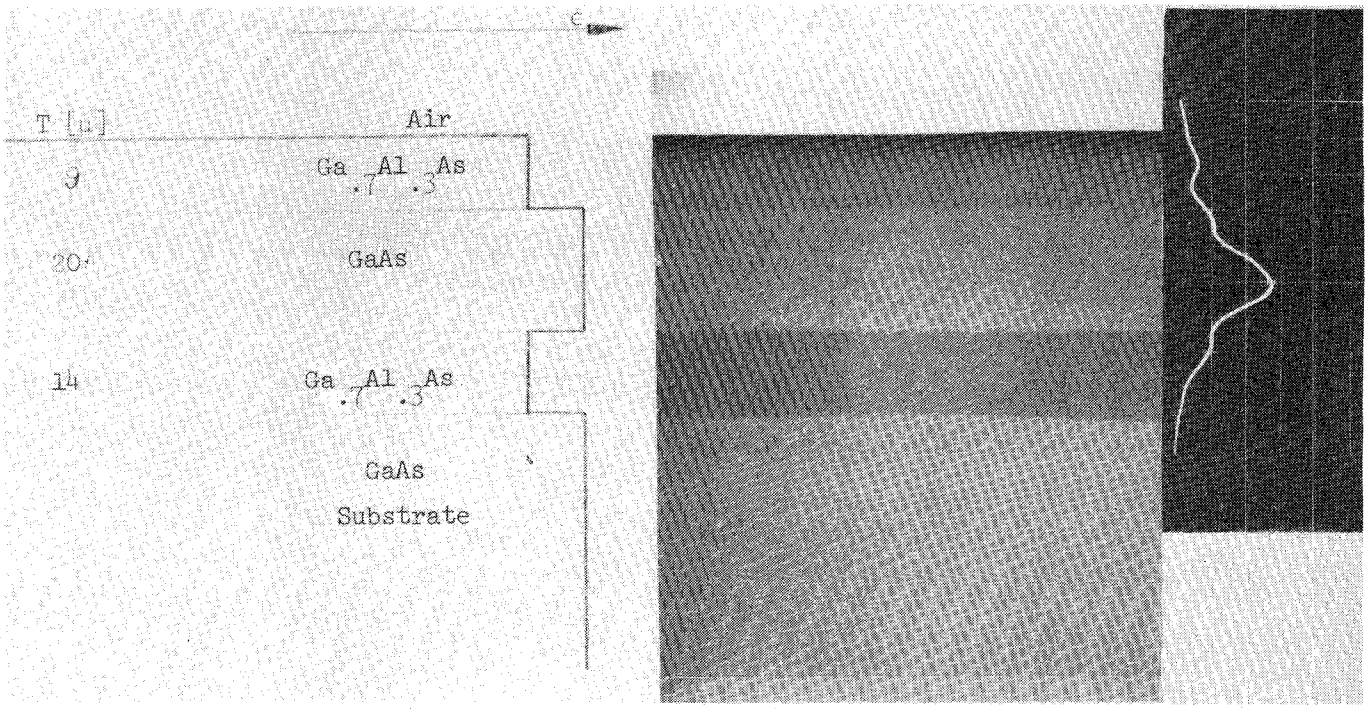

Fig. 11. A multilayer GaAs–GaAlAs dielectric waveguide.

by Chang *et al.* [30]. Electrooptic modulation of 10.6-μm in epitaxially grown waveguides has been demonstrated by Cheo [31]–[33]. The optical waveguide work relevant to Cheo's modulators has been described by Cheo *et al.* [34] and Black *et al.* [35]. The latter work was concerned primarily with the growth and characterization of chromium-doped n-type on n^+-type GaAs thin films. Black *et al.* have grown planar structures with a surface area of 8–10 cm^2 and film thicknesses ranging between 10 and 20 μm with free carrier concentrations in the guiding films reduced to $\leq 10^{12}$ cm^{-3}, Their substrates had free carrier concentrations in the range from 1×10^{17} to 2×10^{18} cm^{-3}.

Work on beam deflection and modulation of 1-μm light in thin film GaAs–(GaAl)As heterostructure waveguides has been reported by McFee *et al.* [36]. The planar heterostructure waveguide itself has been described by McFee *et al.* [37]. In this work substrate epitaxial layers with Al concentrations x ranging between 0.2 and 0.3 were used. The waveguide GaAs layers were 10–20 μm thick and had carrier concentrations of $\sim 10^{16}$ cm^{-3}. Transmission losses of $\sim$2 dB/cm (minimum) were measured.

Since waveguides for 10-μm applications must be relatively thick (i.e., $\sim$10 μm or over in thickness) it is possible to fabricate them from bulk material by grinding, lapping, and polishing. Lotspeich [38] has reported work on 10.6-μm modulators constructed by such techniques. He has fabricated and tested waveguide crystal films ranging in thickness from 8 to 67 μm and observed a propagation loss as low as 0.7 dB/cm for TE polarization.

C. Ion Etched Waveguides

In addition to planar waveguides three dimensional channel shaped waveguides can also be produced in GaAs. The techniques of proton bombardment and ion implantation discussed earlier are particularly suitable for producing channel waveguides since implantation can be done through a mask formed on the surface of the semiconductor. Evaporated gold films ($\sim$2000 Å thick), photoresist masked and ion beam etched to the desired configuration are often used as implantation masks [39].

Alternatively channel guides can be fabricated by direct ion or electron beam etching of thin film planar guides. Such techniques have been employed for fabrication of various configurations of coupled channel guides [40] which can serve as directional couplers. These techniques are quite versatile and can be used to fabricate other integrated optics components such as gratings [41] [42]. The range of their applicability has not yet been fully explored. An example of a channel waveguide ion etched in GaAs is shown in Fig. 12.

Three dimensional guides have also been fabricated by molecular-beam epitaxy (MBE) method [43], [44]. This method can produce an index-of-refraction n_1 region completely surrounded by a medium of index n_2 with $n_1 > n_2$. The MBE method employs GaAs and Al molecular beams to deposit layers of GaAs or (GaAl)As in ultrahigh vacuum. Masking wires or photolithographically generated masks appropriately placed in the modecular beam path can be used to fabricate desired waveguide configurations.

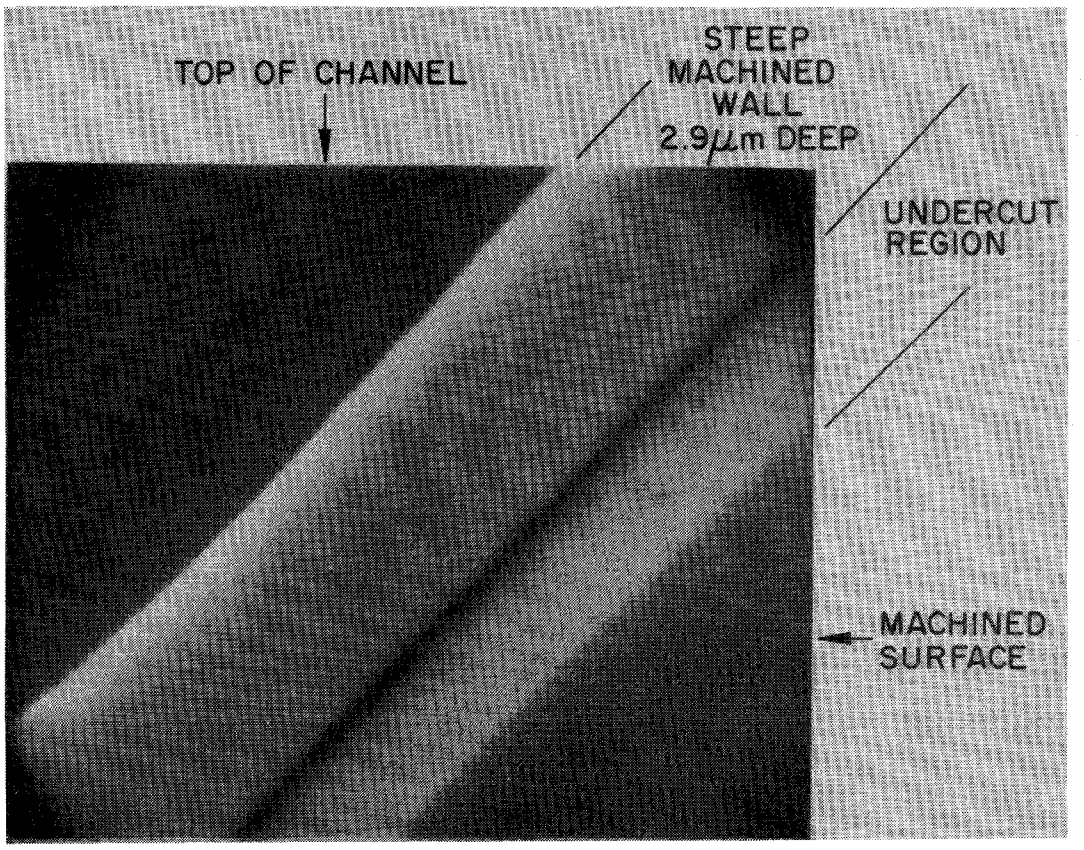

Fig. 12. Scanning electron micrograph of an ion etched channel in GaAs.

III. DIRECTIONAL COUPLING

The principle of directional coupling is well known and directional couplers are an indispensable part of any microwave circuit. These couplers are used in dividing, multiplexing, mixing, and sampling of signals. These devices will play similar roles in the optical circuits of the future.

Directional coupling takes place when two dielectric waveguides, designated as a and b, are in close proximity so that considerable overlap of the mode fields exists. Under these conditions power fed into guide a may be transferred completely or partially into guide b and vice versa [45].

The coupling is described by means of equations of the type

$$\frac{dA}{dz} = \kappa_{ab} B \exp\left[-i(\beta_b - \beta_a)z\right]$$

$$\frac{dB}{dz} = -\kappa_{ab}^* \exp\left[i(\beta_b - \beta_a)z\right] \tag{9}$$

where A and B are the normal mode amplitudes, β_a and β_b are the respective propagation constants, while κ is the coupling coefficient.

The coupling coefficient depends on mode overlap and is given by [46]

$$\kappa_{ab} = -\frac{i\omega\epsilon_0}{4}\int_{-\infty}^{\infty} [n_c^2(x) - n_a^2(x)]\xi_y^{(a)}(x)\xi_y^{(b)}(x)\,dx. \tag{10}$$

Here we assume a slab geometry with $\partial/\partial y = 0$. $n_c^2(x)$ is the actual index (squared) profile of the two-guide system. n_a^2 is the index profile (squared) of guide a alone. $\xi_y^{(a)}(x)$, $\xi_y^{(b)}(x)$ are the normal field distributions of modes a and b.

The solution of (47) for the case of an input at mode B alone, i.e., $A(0) = 0$, $B(0) \equiv B_0$, is

$$A(z) = B_0 \frac{2\kappa_{ab}}{(4\kappa^2 + \Delta^2)^{1/2}} \exp\left(-\frac{i\Delta z}{2}\right) \sin\left[\tfrac{1}{2}(4\kappa^2 + \Delta^2)^{1/2}z\right]$$

$$B(z) = B_0 \exp\left(\frac{i\Delta z}{2}\right)\left\{\cos\left[\tfrac{1}{2}(4\kappa^2 + \Delta^2)^{1/2}z\right]\right.$$

$$\left. - i\frac{\Delta}{(4\kappa^2 + \Delta^2)^{1/2}} \sin\left[\tfrac{1}{2}(4\kappa^2 + \Delta^2)^{1/2}z\right]\right\} \quad [11]$$

where $\kappa \equiv |\kappa_{ab}|$, $\Delta \equiv \beta_b - \beta_a$. Under phase-matched condition, $\Delta = 0$, a complete spatially periodic power transfer between modes a and b takes place with a period $\Delta z = \pi/\kappa$:

$$A(z) = B_0 \frac{\kappa_{ab}}{\kappa} \sin(\kappa z)$$

$$B(z) = B_0 \cos \kappa z \tag{12}$$

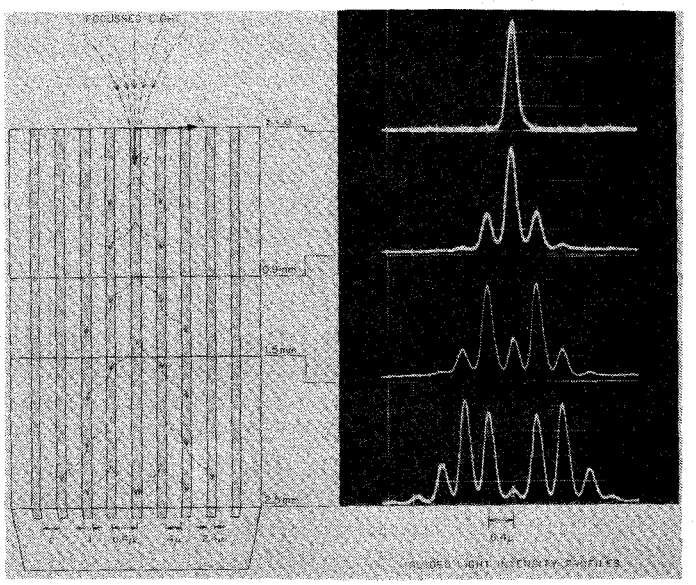

Fig. 13. Directional coupling in a multichannel GaAs waveguide system. After [48].

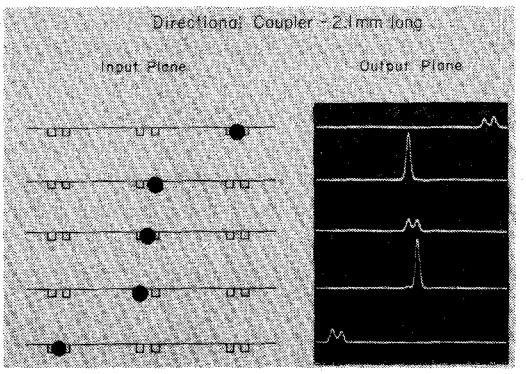

Fig. 14. Directional coupling in isolated pairs of GaAs channel waveguides. After [49].

The first demonstration of directional coupling in channel waveguides took place in a multiwaveguide system [48] such as shown in Fig. 13.

The waveguides were produced by ion implantation through a mask into a heavily doped GaAs crystal as described in Section II. In this multiwaveguide case the coupling is expressed by an infinite set of equations

$$\frac{dA_n}{dz} = -i\kappa A_{n-1} - i\kappa A_{n+1} \tag{13}$$

where n refers to the guide number. If we excite one guide, say $n = 0$, at $z = 0$ so that $A_0(0) = 1$ and $A_{n\neq 0}(0) = 0$, the solution of (13) is

$$A_n(z) = (-i)^n J_n(2\kappa z)$$

where J_n is the Bessel function of order n. The experimental demonstration of such multimode coupling is shown in Fig. 13. Isolated pairs of channel optical waveguides in GaAs have been produced by Somekh *et al.* [49] by both proton implantation and by ion etching. An example of complete power exchange in a two-guide system in a distance of 2.1 mm is shown in Fig. 14 [49].

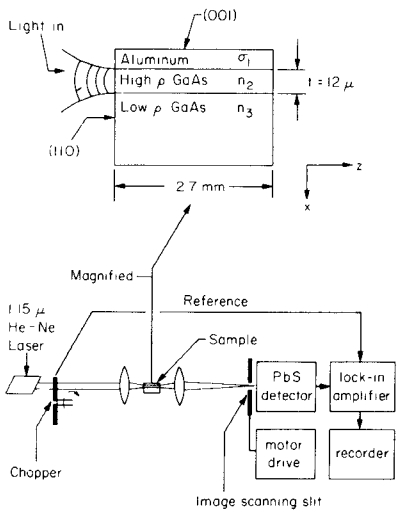

Fig. 15. Schematic diagram of first experimental demonstration of guiding and modulation in epitaxial GaAs waveguides. After [11].

IV. ELECTROOPTIC MODULATION

Two approaches to modulation in GaAs waveguides have been demonstrated. The first, due to Hall *et al.* [11], [12] utilized an epitaxial surface waveguide layer as in Fig. 15. A reverse-biased Schottky barrier due to an evaporated metal electrode provides a high electrical field in the depletion layer which is also the guiding layer. The electrically induced birefringence can then be used for conventional electrooptic amplitude or phase modulation or TE $\leftrightarrow$ TM mode conversion [47].

The second approach demonstrated by Reinhart and Miller [50] involves guiding of light in a heterojunction GaAlAs–GaAs–GaAlAs structure. An applied field will then cause modulation as in the surface waveguide considered earlier.

The main advantage of waveguide modulators compared to bulk modulators is the potentially vastly lower modulation power requirements.

A conventional transverse electrooptic modulator requires a modulation power of [51]

$$P_{\min} = \frac{\epsilon_m \epsilon_0 \lambda_0^3}{n^7 r^2} m^2 B \tag{14}$$

where ϵ_m is the dielectric constant of the modulation frequencies, λ_0 the optical vacuum wavelength, n the index of refraction, r the effective electrooptic coefficient, m the modulation index, and B the information bandwidth.

The fact that $P_{\min}$ is independent of the modulator length is due to the fact that because of diffraction considerations, lengthening of the crystal must be accompanied under optimal focusing conditions by an increase of the beam diameter.

A guided wave modulator, on the other hand, is free of diffraction since the beam is continuously refocused by total internal reflection. The result is that the minimum modulation power is given by

$$P_{\min} = \frac{\pi \lambda_0^2 \epsilon_m \epsilon_0}{4 n^6 r^2} \left(\frac{wt}{l}\right) m^2 B \tag{15}$$

TABLE IV
A Comparison of Bulk and Waveguide Modulation Characteristics

Modulator Type	$Ga_{1-x}Al_xAs$ Thin Film	$LiTaO_3$ Bulk Modulator
t--thickness	1 μm	0.25 mm
w--width	10 μm	0.25 mm
L--length	1 cm	1 cm
ϵ_m--dielectric constant	11	43
λ--optical wavelength	8500 Å	6328 Å
B--bandwidth	100 MHz	100 MHz
V--modulator voltage for m = 40%	0.1 V	9 V
P--power for 40% AM	0.02 mW	60 mW

where w,t are the transverse dimensions of the channel guide whose length is l.

A comparison of the modulation power requirements of a typical bulk and a waveguide modulator are shown in Table IV.

It is clear that one may expect 2–3 orders of magnitude reduction in the modulation power requirement in optimally designed waveguide modulators.

Before closing this section we should mention the extensive work of Cheo and coworkers on 10.6-μm modulation in GaAs epitaxial waveguides [31]–[35].

V. INTEGRATED DETECTORS

Bombardment of GaAs with high energy protons can be used advantageously in the fabrication of optical detectors. Proton bombardment causes an absorption edge shift to energy low enough to permit detection of photons which can be guided with little absorption in waveguides formed in the GaAs by any of the usual methods.

This technique for fabricating optical waveguide detectors in GaAs has been reported by Stoll *et al.* [52]. In their work they used a configuration shown in Fig. 16. A small volume of epitaxial GaAs waveguide was implanted with protons. Structural disorder created by the implantation process causes the previously low-loss waveguide to become highly lossy for radiation around 1 μm. One of the mechanisms responsible for this absorption is the liberation of free carriers which had become trapped at defect centers. A photodetector results when these carriers

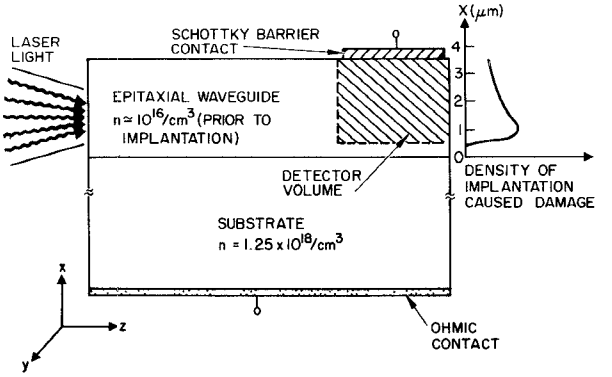

Fig. 16. The proton implanted GaAs waveguide detector. After [52].

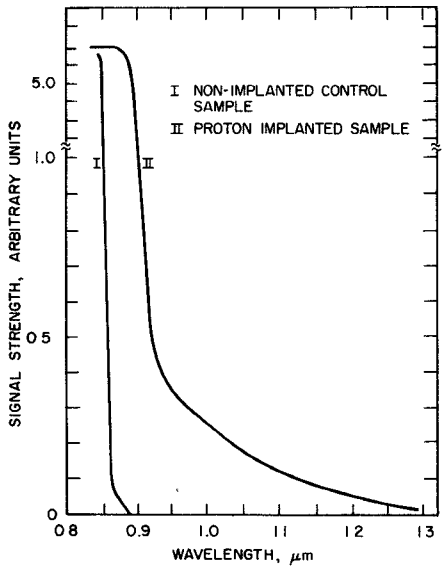

Fig. 17. The photoresponse of a proton implanted GaAs waveguide detector. After [52].

are swept through the depletion layer generated by a reverse-biased Schottky barrier which has been deposited over the implanted region as shown in Fig. 16. The detectors were found to be sensitive to light of wavelengths >0.9 μm, a wavelength which can be transmitted nearly unattenuated by the GaAs guides used. The optical waveguide structure consisted of a 3.5-μm-thick n-type (S-doped, $n \simeq 10^{18}/\text{cm}^3$) epitaxial film grown on a degenerate n-type substrate ($n \simeq 1.25 \times 10^{18}/\text{cm}^3$). Prior to proton implantation optical attenuation at 1.15 μm was measured to be 1.3 cm^{-1}. The detector volume was proton bombarded to form the waveguide detector, 300-keV protons were used, the total integrated flux of which was $2 \times 10^{15}/\text{cm}^2$. The damage layer which resulted was approximately 3 μm thick with a damage peak occurring about 2.5 μm below the surface. The implanted waveguide was then annealed at 500°C for 30 min in order to allow some optical transmission through the damaged region. Finally, 11-mils^2 Al Schottky barriers were evaporated in a waffle pattern over the implanted area.

Upon the application of a sufficient reverse bias to the Schottky barrier, a depletion layer is produced which extends across the high-resistivity waveguiding layer to the lower resistivity substrate. Any dipole transitions made possible by radiation-produced defect levels generate free carriers which are swept out of the depletion layer, thereby causing current to flow through an external circuit. Measurements of the photosensitivity of both unimplanted and implanted annealed samples are shown in Fig. 17. Transparent Au barriers, sputter deposited on the surface, were used to measure sensitivity as a function of wavelength. The curve for the irradiated sample reveals a defect associated energy level distribution within the band gap, as well as a shift of the effective absorption edge to lower energies. Stoll *et al.* [52] report that substantially all of the implantation-induced optical attenuation in the 1-μm wavelength region can be attributed to absorption as opposed to diffuse scattering.

The response time of the proton implanted detector was determined to be shorter than 200 ns, the measurement being limited by the duration of the Nd:YAG Q-switched pulses used in the measurement.

Fabrication of a proton implanted detector integrally within a GaAlAs waveguide can be accomplished by using the same techniques that have been applied successfully to GaAs. Probably the most useful integral waveguide/detector combination would be one that could function satisfactorily at a wavelength of 0.9 μm, and, hence could be used with a GaAs LED or laser source. A more detailed study of proton implanted GaAs detectors and the physical mechanisms involved has been performed by Stoll *et al.* [53].

A different approach to integrated waveguide detectors has been taken by Stillman *et al.* [54]. They have fabricated $In_xGa_{1-x}As$ avalanche photodiodes and integrated them into high-purity epitaxial GaAs waveguides which were 10–20 μm thick and were grown on n^+ GaAs substrates.

$In_xGa_{1-x}As$ was grown epitaxially on the n^+ substrates through holes etched in the high-purity GaAs epitaxial layer. The grown areas in $In_xGa_{1-x}As$ were about 5 mils in diameter and were polished flush with the surface of the GaAs waveguide. In concentration was $x = 0.20$ so that the devices would be suitable for the detection of 1.06-μm guided radiation.

Stillman *et al.* reported a 60-percent quantum efficiency for the $In_xGa_{1-x}As$ detectors. In the discrete version of these detectors avalanche gains as high as 250 were measure with rise times of 170 ps. By adjusting the composition of the ternary alloy peak response of the diodes could be varied between 0.85 and 3.5 μm. The main limitation of $In_xGa1_{-x}As$ as a material for other integrated optics application is the lattice mismatch between GaAs and the alloy, which becomes 7.2 percent for 100 percent InAs. This degrades the crystalline quality of the material. However, epitaxial growth techniques to minimize this problem are being pursued [55].

VI. LASER SOURCES

The CW GaAs–GaAlAs heterojunction lasers [8]–[10] seem ideally suited to act as sources for integrated optics. The epitaxial technology used to fabricate them is similar to that used to make most of the other components described earlier. The intense effort to develop and extend the lifetime of these lasers is taking place independently of the research in integrated optics and is described adequately elsewhere [56], [57].

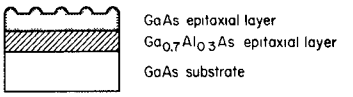

Fig. 18. A GaAs–GaAlAs epitaxial laser with corrugation feedback. After [59].

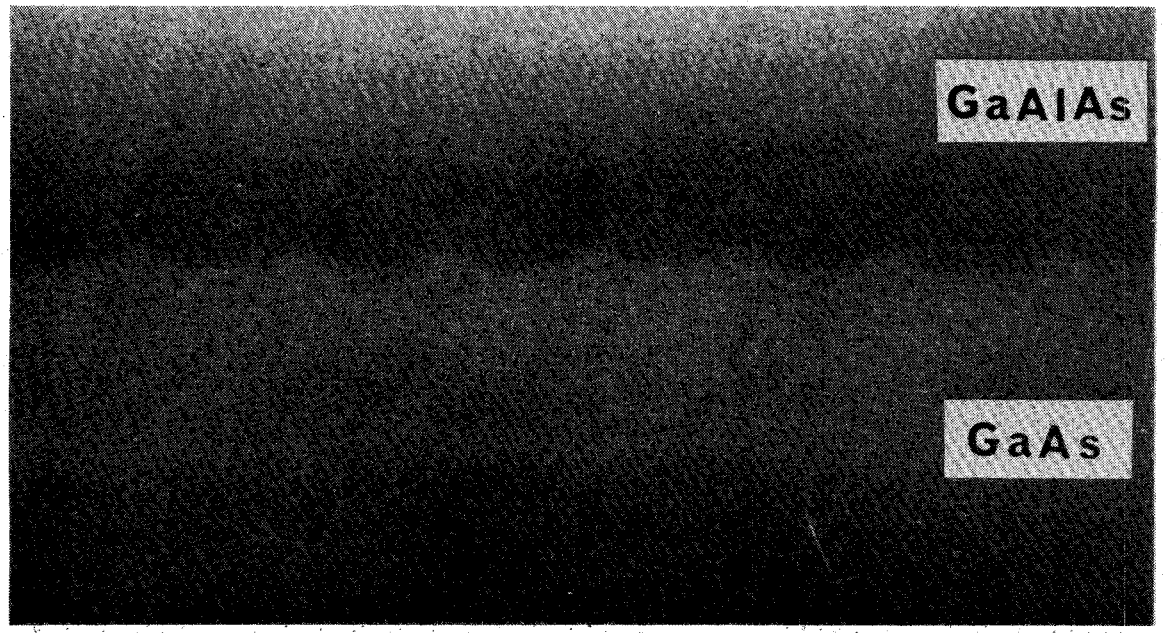

Fig. 19. An epitaxial film of $Ga_{0.5}Al_{0.5}As$ grown on top of a corrugated GaAs substrate. Period = 0.347 μm. After [62].

The corrugated GaAs laser [58], [59] possesses some unique properties which lend themselves to integrated optics applications. The need for end reflectors, which are difficult to fabricate on a monolithic single crystal chip, is obviated by incorporating a corrugation on one of the interfaces adjacent to the active (amplifying) medium.

The period Λ of the corrugation is chosen to satisfy

$$\frac{\pi}{\Lambda} = \beta, \qquad m = 1,2,3\cdots \tag{16}$$

i.e., Λ is equal to an integer times a half guide wavelength. The theory and first demonstration of such lasers (in organic dyes) is due to Kogelnik and Shank [60].

In the case of GaAs lasers a convenient technique for producing this feedback is by corrugating an interface of the dielectric laser waveguide as in Fig. 18.

The corrugation period for fundamental feedback ($m = 1$) in GaAs is $\Lambda \approx 1100$ Å. Such corrugations have been produced by ion etching the surface through a photoresist mask [40]. The mask is made by exposure to the interference pattern of two oppositely traveling beams split off from the same He-Cd laser [61].

More recent work demonstrated [62] that it is possible to grow high quality GaAs or GaAlAs on corrugated surfaces as shown in Fig. 19. This led to electrical double heterostructure injection lasers with internal corrugation feedback [63].

One of the main advantages from corrugation feedback GaAs lasers is the prospect of both longitudinal [60] and transverse mode control which it affords. The oscillation frequency is determined by the corrugation period through relation (16). This is illustrated by the experimental data of Fig. 20 obtained from an optically pumped laser as shown in Fig. 18.

Another potential solution to the fabrication of laser sources on integrated optics chips is the mesa surface

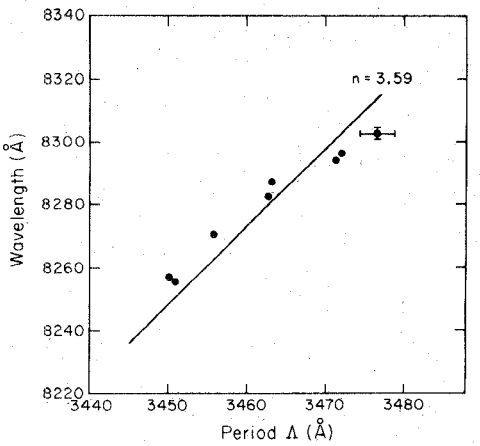

Fig. 20. The dependence of the oscillation wavelength of a GaAs corrugated laser on the corrugation period. After [59].

laser described recently by Scott *et al.* [64]. They succeeded in growing a mesa with parallel sets of {111} planes which possess a high degree of surface flatness.

In more recent still unpublished work the same authors and F. Blum succeeded in operating the mesa as an injection laser.

Another important development in this area is the demonstration by Barnoski *et al.* [65] of laser action in GaAs in which one of the dopants is introduced by ion implantation. Ion implantation through masks similar to those used for ion etching of currugated lasers can lead to a new family of injection modulated lasers.

VII. APPROACHES TO CIRCUIT INTEGRATION AND POTENTIAL APPLICATIONS

The purpose of an OIC is to perform functions with light that the present systems perform electrically, while still retaining the reliability, low cost, and small size and weight of an electrical integrated circuit. Thus it is de-

sirable in the long run to achieve as high a degree of integration of the various components as possible.

There are, at present, two approaches one can take in order to achieve this goal. One is the monolothic circuit approach in which all the components are fabricated using basically the same material (such as $Ga_{1-x}Al_xAs$ with varying values of x) on a single chip substrate. This approach is very attractive in the long run but is somewhat ambitious for the present state of development of integrated optics technology. As we have already seen, many of the individual devices which could serve as components in a monolithic integrated circuit have been fabricated and demonstrated in the laboratory. However, the several elements have not yet been integrated onto a single chip to produce an operational OIC.

The other approach to OIC development consists of fabricating individual integrated circuit components using materials best suited for a given device as known at this time, and integrating these into a circuit using materials not necessarily similar to the ones used for the components. This approach complicates the problem of coupling between various components and guides but is probably more practically realizable in the short term. Many of the components now being developed are compatible with either of the two preceding approaches. For the monolithic circuit approach the $GaAs/Ga_{1-x}Al_xAs$ system seems to be the most promising since it offers the possibility of wavelength compatibility.

In either case one of the long term objectives is the development of technologies and components, eventual integration of these components into optical circuits, and coupling of these circuits with low-loss single mode fibers. The resulting communication systems can in principle provide length–bandwidth (bit rate) products in the gigabit-kilometer range. Low-loss single mode glass fiber waveguides are currently available at the research level [66]. Applications other than communication systems may also be ultimately possible. It is anticipated that OIC's will be useful in systems such as optical radars, signal processors, multiplexers, and optical data links.

ACKNOWLEDGMENT

The authors would like to acknowledge the invaluable contributions of R. G. Hunsperger and M. K. Barnoski, who provided a number of unpublished reports, figures, and comments to assist in the preparation of the present paper.

REFERENCES

[1] a) E. A. J. Mercatili and L. A. Schmeltzer, "Hollow metallic and dielectric waveguides for long distance optical transmission and lasers," *Bell Syst. Tech. J.*, vol. 43, p. 1783, 1964.
b) H. Steffen and F. K. Kneubühl, "Dielectric tube resonators for infrared and submillimeterwave lasers," *Phys. Lett.*, vol. 27A, p. 612, 1968.
c) P. W. Smith, "A waveguide gas laser," *Appl. Phys. Lett.*, vol. 19, p. 132, 1971.
d) R. L. Abrams and W. B. Bridges, "Characteristics of sealed-off waveguide CO_2 lasers," *IEEE J. Quantum Electron.*, vol. QE-9, pp. 940–946, Sept. 1973.

[2] R. N. Hall *et al.*, "Coherent light emission from GaAs junctions," *Phys. Rev. Lett.*, vol. 9, p. 366, 1962.

[3] M. I. Nathan *et al.*, "Stimulated emission of radiation from GaAs p-n junctions," *Appl. Phys. Lett.*, vol. 1, p. 62, 1962.

[4] A. Yariv and R. C. C. Leite, "Dielectric waveguide mode of light propagation in p-n junctions," *Appl. Phys. Lett.*, vol. 2, p. 55, 1963.

[5] W. C. Bond, B. G. Cohen, R. C. C. Leite, and A. Yariv, "Observation of the dielectric mode waveguide of light propagation in p-n junctions," *Appl. Phys. Lett.*, vol. 2, p. 57, 1963.

[6] D. F. Nelson and F. K. Reinhart, "Light modulation by the electrooptic effect in GaP junctions," *Appl. Phys. Lett.*, vol. 2, p. 55, 1964.

[7] H. Kroemer, "Quasielectric and quasi-magnetic fields in non-uniform semiconductors," *RCA Rev.*, vol. 18, p. 332, 1957.

[8] Z. I. Alferov *et al.*, "Coherent radiation of epitaxial heterojunction structures in the AlAs-GaAs system," *Sov. Phys.—Semicond.*, vol. 2, p. 1289, 1969.

[9] H. Kressel and H. Nelson, "Close confinement GaAs p-n junction laser with reduced optical loss at room temperature," *RCA Rev.*, vol. 30, p. 106, 1969.

[10] I. Hayashi, M. B. Panish, and P. W. Foy, "A low-threshold room-temperature injection laser," *IEEE J. Quantum Electron.*, vol. QE-5, pp. 211–212, Apr. 1969.

[11] D. Hall, A. Yariv, and E. Garmire, "Optical guiding and electrooptic modulation in GaAs epitaxial films," *Opt. Commun.*, vol. 1, p. 403, 1970.

[12] ——, "Observation of propagation cutoff and its control in thin film optical waveguides," *Appl. Phys. Lett.*, vol. 17, p. 127, 1970.

[13] S. E. Miller, "Integrated optics, an introduction," *Bell Syst. Tech. J.*, vol. 48, p. 2059, 1969.

[14] R. E. Collin, *Field Theory of Guided Waves*. New York: McGraw-Hill, 1960, p. 470.

[15] E. Garmire, H. Stoll, A. Yariv, and R. G. Hunsperger, "Optical waveguiding in proton-implanted GaAs," *Appl. Phys. Lett.*, vol. 21, p. 87, 1972.

[16] A. G. Foyt, W. T. Lindley, C. M. Wolfe, and J. P. Donnelly, "Isolation of junction devices in GaAs using proton bombardment," *Solid-State Electron.*, vol. 12, p. 209, 1969.

[17] H. Stoll and R. G. Hunsperger, private communication.

[18] E. Garmire *et al.*, presented at the Device Research Conf., Edmonton, Alta., Canada, June 22, 1972.

[19] H. C. Casey, Jr., D. D. Sell, and M. B. Panish, "Refractive index of $Al_xGa_{1-x}As$ between 1.2 and 1.8 eV," *Appl. Phys. Lett.*, vol. 24, p. 633, 1974.

[20] H. Kressel, H. F. Lockwood, and H. Nelson, "Low-threshold $Al_xG_{1-x}As$ visible and IR-light-emitting diode lasers," *IEEE J. Quantum Electron. (Special Issue on Semiconductors)*, vol. QE-6, pp. 278–284, June 1970.

[21] J. Shah, B. I. Miller, and A. E. DiGiovanni, "Photoluminescence of $Al_xGa_{1-x}As$," *J. Appl. Phys.*, vol. 43, p. 3436, 1972.

[22] W. G. Spitzer and S. M. Whelan, "Infrared absorption and electron effective mass in n-type gallium arsenide," *Phys. Rev.*, vol. 14, p. 59, 1959.

[23] G. S. Kamath *et al.*, "Integrated optics," Semiannual Tech. Rep. 2, Contract F19628-72-C-0322, AFCRL-TR-0713, Aug. 1973.

[24] J. T. Boyd, "Theory of parametric oscillation phase matched in GaAs thin-film waveguides," *IEEE J. Quantum Electron.*, vol. QE-8, pp. 788–796, Oct. 1972.

[25] M. D. Sturge, "Optical absorption of gallium arsenide between 0.6 and 2.75 eV," *Phys. Rev.*, vol. 127, p. 768, 1962.

[26] M. G. Craford and W. O. Groves, "Vapor phase epitaxial materials for LED applications (*Invited Paper*)," *Proc. IEEE (Special Issue on New Materials for Display Devices)*, vol. 61, pp. 862–880, July 1973.

[27] E. Garmire, "Optical waveguides in single layers of $Ga_{1-x}Al_xAs$ grown on GaAs substrates," *Appl. Phys. Lett.*, vol. 23, p. 403, 1973.

[28] S. Kamath, in *Dig. Tech. Papers, Topical Meeting Integrated Optics* (New Orleans, La.), Jan. 1974.

[29] W. S. C. Chang and K. W. Loh, "Theoretical design of guided wave structure of electrooptic modulation at 10.6 μm," *IEEE J. Quantum Electron.*, vol. QE-8, pp. 463–470, June 1972.

[30] W. S. C. Chang *et al.*, in *Dig. Tech. Papers, Topical Meeting Integrated Optics* (New Orleans, La.), Jan. 1974.

[31] P. K. Cheo, "Pulse amplitude modulation of a CO_2 laser in electrooptic thin-film waveguide," *Appl. Phys. Lett.*, vol. 22, p. 241, 1973.

[32] ——, "Electrooptic properties of reverse-biased GaAs epitaxial thin films at 10.6 μm," *Appl. Phys. Lett.*, vol. 23, p. 439, 1973.

[33] ——, in *Dig. Tech. Papers, Topical Meeting Integrated Optics* (New Orleans, La.), Jan. 1974.

[34] P. K. Cheo, J. M. Berak, W. Oshinsky, and J. L. Swindal, "Optical waveguide structures for CO_2 lasers," *Appl. Opt.*, vol. 12, p. 500, 1973.

[35] J. F. Black, J. L. Swindal, and P. K. Cheo, in *Dig. Tech. Papers, Topical Meeting Integrated Optics* (New Orleans, La.), Jan. 1974.

[36] J. H. McFee, R. E. Nahory, M. A. Pollack, and R. A. Logan, "Beam deflection and amplitude modulation of 10.6 μm guided waves by free-carrier injection in GaAs-AlGaAs heterostructures," *Appl. Phys. Lett.*, vol. 23, p. 571, 1973.
[37] J. H. McFee, M. A. Pollack, W. W. Rigrod, and R. A. Logan, in *Dig. Tech. Papers, Topical Meeting Integrated Optics* (New Orleans, La.), Jan. 1974.
[38] J. F. Lotspeich, in *Dig. Tech. Papers, Topical Meeting Integrated Optics* (New Orleans, La.), Jan. 1974.
[39] H. L. Garvin *et al.*, "Integrated optics and guided waves—A report of the Topical Meeting," *Appl. Opt.*, vol. 11, p. 1675, 1972.
[40] H. L. Garvin *et al.*, "Ion beam micromachining of integrated optic components," *Appl. Opt.*, vol. 12, p. 455, 1973.
[41] A. Yariv, "Components for integrated optics," *Laser Focus*, Dec. 1972.
[42] J. J. Turner *et al.*, "Gratings for integrated optics fabricated by electron microscope," *Appl. Phys. Lett.*, vol. 23, p. 333, 1973.
[43] A. Y. Cho and F. K. Reinhart, "Growth of three dimensional dielectric waveguides for integrated optics of molecular-beam epitaxy method," *Appl. Phys. Lett.*, vol. 21, p. 355, 1972.
[44] J. C. Tracy, W. Weigman, R. A. Logan, and F. K. Reinhart, "Three-dimensional light guides in single-crystal Ga-As-$Al_xGa_{1-x}As$," *Appl. Phys. Lett.*, vol. 22, p. 511, 1973.
[45] W. H. Louisell, *Coupled Modes and Parametric Electronics*. New York: Wiley, 1960.
[46] S. Somekh, "Theory, fabrication and performance of some integrated optical devices," Ph.D. dissertation, California Inst. Technol., Pasadena, 1974.
[47] A. Yariv, "Coupled-mode theory for guided-wave optics," *IEEE J. Quantum Electron.*, vol. QE-9, pp. 919–933, Sept. 1973.
[48] S. Somekh, E. Garmire, and A. Yariv, "Channel optical waveguiding directional couplers," *Appl. Phys. Lett.*, vol. 22, p. 46, 1973.
[49] S. Somekh *et al.*, "Channel optical waveguides and directional couplers in GaAs-imbedded and ridged," *Appl. Opt.*, vol. 13, p. 327, 1974.
[50] F. K. Reinhart and B. I. Miller, "Efficient GaAs-$Al_xGa_{1-x}As$ modulators," *Appl. Phys. Lett.*, vol. 20, p. 36, 1972.
[51] A. Yariv, *Introduction to Optical Electronics*. New York: Holt, Rinehart and Winston, 1971, p. 326.
[52] H. Stoll, A. Yariv, R. G. Hunsperger, and G. L. Tangonan, "Proton-implanted optical waveguide detectors in GaAs," *Appl. Phys. Lett.*, vol. 23, p. 664, 1973.
[53] H. Stoll, A. Yariv, and R. G. Hunsperger, to be published.
[54] G. E. Stillman, C. M. Wolfe, and I. Melngailis, "Monolithic integrated $In_xGa_{1-x}As$ Schottky barrier waveguide detector," in *Dig. Tech. Papers, Topical Meeting Integrated Optics* (New Orleans, La.), Jan. 1974.
[55] C. M. Wolfe, G. E. Stillman, and I. Melngailis, in *Dig. Tech. Papers, Topical Meeting Integrated Optics* (New Orleans, La.), Jan. 1974.
[56] W. D. Johnston, Jr., and B. I. Miller, "Degradation characteristics of CW $Al_xGa_{1-x}As$ heterostructure lasers," *Appl. Phys. Lett.*, vol. 23, p. 192, 1973.
[57] H. Yonezu *et al.*, "Degradation mechanism of (Al–Ga)As double heterostructure laser diodes," *Appl. Phys. Lett.*, vol. 24, p. 18, 1974.
[58] M. Nakamura, A. Yariv, H. W. Yen, and S. Somekh, "Optically pumped GaAs surface laser with corrugation feedback," *Appl. Phys. Lett.*, vol. 22, p. 515, 1973.
[59] M. Nakamura *et al.*, "Laser oscillation in epitaxial GaAs waveguides with corrugation feedback," *Appl. Phys. Lett.*, vol. 23, p. 224, 1973.
[60] H. Kogelnik and C. V. Shank, "Coupled wave theory of distributed feedback lasers," *J. Appl. Phys.*, vol. 43, p. 2327, 1972.
[61] H. W. Yen *et al.*, "Optically pumped GaAs waveguide lasers with a fundamental 0.11 μm corrugation feedback," *Opt. Commun.*, vol. 9, p. 35, 1973.
[62] M. Nakamura *et al.*, "Liquid phase epitaxy of GaAlAs on GaAs substrates with fine surface corrugations," *Appl. Phys. Lett.*, May 1974. (Similar results were reported at the New Orleans Topical Meeting on Integrated Optics 1974 by Schmidt, Shank, and Miller of Bell Laboratories and by Bannantyne and Tang of Cornell University.)
[63] M. Nakamura, K. Aiki, Jun-Ichi Umeda, A. Yariv, H. W. Yien, and T. Morikawa, "GaAs-$Ga_{1-x}Al_xAs$ double heterostructure distributed feedback diode lasers," *Appl. Phys. Lett.*, vol. 25, pp. 487–488, Nov. 1974.
[64] W. C. Scott, K. L. Lawley, and W. C. Holton, "Mesa surface laser," in *Dig. Tech. Papers, Topical Meeting on Integrated Optics* (New Orleans, La.), Jan. 1974.
[65] M. K. Barnoski, R. G. Hunsperger, and A. Lee, "Ion implanted GaAs injection laser," in *Dig. Tech. Papers, Topical Meeting Integrated Optics* (New Orleans, La.), Jan. 1974.
[66] D. B. Keck, R. D. Maurer, and P. C. Schultz, "On the ultimate lower limit of attenuation in glass optical fibers," *Appl. Phys. Lett.*, vol. 22, p. 307, 1973.

Optical Waveguide Modulators

IVAN P. KAMINOW, FELLOW, IEEE

(Invited Paper)

***Abstract*—A tutorial survey of recent work on optical waveguide modulators in electrooptic, acoustooptic, and magnetooptic materials is presented. Methods for realizing waveguiding layers in modulating materials and various modulator configurations are considered.**

I. INTRODUCTION

HIGH-speed light modulators and beam deflectors that make use of the electrooptic, acoustooptic, magnetooptic, and electroabsorption effects in bulk materials have been described in several reviews [1]–[5]. The first three effects produce refractive index changes in response to the appropriate modulating electric, acoustic, and magnetic fields. The last effect produces a change in optical absorption in response to an electric field.

The performance of these modulators is often specified in terms of μ, the electrical modulating power P required to produce a given degree of modulation over a bandwidth Δf. The performance depends upon optical wavelength λ, the properties of the modulating material, and the device geometry. One of the chief advantages an optical waveguide modulator has over the conventional bulk modulator, is the substantial improvement in the geometrical factor allowed by the confinement of the optical beam to a small cross section over an extended length.

Manuscript received April 19, 1974; revised July 11, 1974.
The author is with the Bell Telephone Laboratories, Crawford Hill Laboratory, Holmdel, N. J. 07733.